Progress in Nuclear Energy 148 (2022) 104233

Contents lists available at ScienceDirect

Progress in Nuclear Energy

journal homepage: www.elsevier.com/locate/pnucene

Frequency-domain models in the SP_N approximation for neutron noise calculations

A. Carreño [a], A. Vidal-Ferràndiz [b], D. Ginestar [b], G. Verdú [a,*]

[a] Instituto Universitario de Seguridad Industrial, Radiofísica y Medioambiental, Universitat Politècnica de València, Camino de Vera, s/n, 46022, València, Spain
[b] Instituto Universitario de Matemática Multidisciplinar, Universitat Politècnica de València, Camino de Vera, s/n, 46022, València, Spain

ARTICLE INFO

Keywords:
Frequency domain
Neutron noise
Simplified spherical harmonics equations
Finite element method

ABSTRACT

Simulations of the neutron flux fluctuations, known as neutron noise, can be performed by means of the spherical harmonics equations (SP_N) approximation with higher accuracy than with the diffusion equation. In this sense, one can solve these equations in the time-domain or in the frequency-domain. This last approach permits solving the neutron noise without performing complete time-dependent simulations for monochromatic perturbations. This work presents two formulations of the SP_N equations in the frequency domain, that are obtained by using different treatments of the time derivatives of the field moments. The methodology is verified with several neutron noise problems where the numerical results are compared with the time-domain computations of `FEMFFUSION` code. The `C5G7` noise benchmark compares both SP_N formulations, showing the applicability of the diffusive SP_N approximation.

1. Introduction

Nowadays, non-invasive detection of anomalies in nuclear power plants is possible through neutron noise monitoring. The early detection of such anomalies gives the possibility to take proper actions before they lead to safety concerns or impact on the plant availability. In this context, neutron noise is studied to analyse the effects of small perturbations in nuclear reactors that are generally produced by stochastic fluctuations of the coolant properties, such as its density or temperature, and mechanical vibration of fuel elements, controls rods and other structures in the reactor. Normally, these fluctuations are expressed as perturbations in the cross-sections of the materials of the reactor.

Over the years, using analytical techniques for simplified problems (Pázsit and Analytis, 1980; Demazière, 2019) or the neutron diffusion equation, spatially discretized with finite difference methods, nodal methods or finite element methods (Demazière and Pázsit, 2009; Rouchon et al., 2017a; Vidal-Ferràndiz et al., 2020c), have provided accurate enough results for neutron noise analysis. However, recent realistic neutron noise benchmarks require better approximations of the neutron transport equations with the capability for simulating strong changes in the flux gradient (Stacey, 2007; Vinai et al., 2021b). For this purpose, currently, the efforts are focused on the application of Monte Carlo methods (Rouchon et al., 2017b) or higher approximations of the neutron transport equation such as the discrete ordinates method, S_N equations, (Yi et al., 2021), spherical harmonics equations, P_N equations, (Larsson and Demazière, 2009). These approximations, even though they provide very accurate results, have an enormous computational cost.

An alternative to these equations is using the simplified spherical harmonics equations, SP_N equations, (Gelbard, 1960; McClarren, 2010). They are a simplification of the P_N equations that can be seen as a generalization of the neutron diffusion equation. In the time-dependent SP_N equations, one can obtain different types of formulations by neglecting or not the time derivatives of the moments (Carreño et al., 2021). In this work, we consider two different approaches: the full formulation, where none of the time derivatives are removed; and the diffusive formulation, where only the time derivatives of the even moments are kept in the expressions. Some works have been devoted to prove that the SP_N improves the results of the neutron diffusion equation for static problems and some transient problems (Hamilton and Evans, 2015; Vidal-Ferràndiz et al., 2019a; Carreño et al., 2021). For neutron noise computations, the diffusive SP_3 equations have shown to be a better approximation than the diffusion equation (Gong et al., 2021).

Once the type of approximation of the neutron transport is chosen, two types of approaches can be applied: neutron noise analysis in the time-domain or in the frequency-domain. In time-domain analysis, the equations can be integrated by using time discretization schemes, quasi-static methods or modal methods among others (Ginestar et al., 1998; Dulla et al., 2008; Carreño et al., 2019). Another possibility is

* Corresponding author.
E-mail address: gverdu@iqn.upv.es (G. Verdú).

https://doi.org/10.1016/j.pnucene.2022.104233
Received 30 November 2021; Received in revised form 25 February 2022; Accepted 8 April 2022

to apply the Method of Characteristics (MOC) to avoiding the need of a spatial homogenization (Gammicchia et al., 2020). In the frequency-domain the neutron flux is decomposed into the steady-state flux and the fluctuation to obtain the neutron noise formulation, and then apply the Fourier transform (Mylonakis et al., 2021; Rouchon et al., 2017a). Several works have compared both formulations (Viebach et al., 2019; Olmo-Juan et al., 2019; Vidal-Ferràndiz et al., 2020c). Usually, the computational simulations with frequency-domain equations are much quicker than if the time-domain equations are used for describing the effect of a perturbation.

The aim of this work is developing the neutron noise multigroup SP_N equations in the frequency-domain for two types of formulations: the full and the diffusive, (Carreño et al., 2021). First-order neutron noise approximations are used, which remove the second order terms related to the fluctuations of the different fields and magnitudes appearing in the equations. Both formulations are compared, showing the applicability of each one of them. To verify the frequency-domain methodology, the results are compared with time-domain results obtained from the `FEMFFUSION` code (Vidal-Ferràndiz et al., 2020b), where a backward difference method is applied for the time discretization.

The structure of the rest of the paper is as follows. Section 2 exposes the neutron noise full SP_N problem in the time-domain, and it also develops this problem for the frequency-domain. In the same way, Section 3 describes the neutron noise diffusive SP_N problem in the time-domain, and it derives the noise problem in the frequency-domain. Section 4 tests the performance of the two SP_N formulations in the frequency-domain using two benchmark problems. First, a simple one-dimensional neutron noise benchmark and second, the 2D neutron noise C5G7 problem. Section 5 closes this paper with the main conclusions obtained.

2. Neutron noise in the full SP_N approximation (FSP_N)

Generally, the simplified spherical harmonics equations (SP_N equations) are derived from the one-dimensional spherical harmonics equation (P_N equations) when the spatial derivatives are substituted by gradients (Stacey, 2007; Olbrant et al., 2013; Chao, 2016; Sanchez, 2019). Different assumptions on the time derivatives of the neutron moments yield different formulations of the time-dependent SP_N equations (Lee et al., 2015; Carreño et al., 2021). This Section derives the full SP_N equations in the frequency-domain (FSP_N-FD equations) from the full SP_N equation in the time-domain (FSP_N-TD equations), which takes into account all time-derivatives of the neutron moments. The FSP_N-TD equations can be expressed as (Carreño et al., 2021),

$$\begin{aligned}&\mathcal{V}\frac{\partial}{\partial t}\boldsymbol{\Phi}^n+\nabla\left(\frac{n}{2n+1}\boldsymbol{\Phi}^{n-1}+\frac{n+1}{2n+1}\boldsymbol{\Phi}^{n+1}\right)+\Sigma^n\boldsymbol{\Phi}^n\\&=\delta_{n,0}\left((1-\beta)\mathcal{R}^p\mathcal{F}\boldsymbol{\Phi}^0+\sum_{k=1}^{K}\lambda_k\mathcal{R}_k^dC_k\right),\quad n=0,1,\dots,N,\end{aligned}\tag{1}$$

where $\delta_{n,0}$ is the Kronecker delta that is equal to 1 only if $n=0$ and zero in other cases. Note that for $n=0$ the term with $\boldsymbol{\Phi}^{n-1}$ cancels out.

The equations for the delayed neutron precursor concentration are

$$\frac{\partial}{\partial t}C_k=-\lambda_kC_k+\beta_k\mathcal{F}\boldsymbol{\Phi}^0,\qquad k=1,\dots,K,\tag{2}$$

where

$$\boldsymbol{\Phi}^n=\left(\boldsymbol{\Phi}_1^n,\boldsymbol{\Phi}_2^n,\dots,\boldsymbol{\Phi}_G^n\right)^T,\quad \mathcal{F}=\begin{pmatrix}\nu_1\Sigma_{f1}&\nu_2\Sigma_{f2}&\dots&\nu_G\Sigma_{fG}\end{pmatrix},\tag{3}$$

$$\Sigma^n=\begin{pmatrix}\Sigma_{t1}-\Sigma_{s11}^n&-\Sigma_{s21}^n&\dots&-\Sigma_{sG1}^n\\-\Sigma_{s12}^n&\Sigma_{t2}-\Sigma_{s22}^n&\dots&-\Sigma_{sG2}^n\\\vdots&\vdots&\ddots&\vdots\\-\Sigma_{s1G}^n&-\Sigma_{s2G}^n&\dots&\Sigma_{tG}-\Sigma_{sGG}^n\end{pmatrix},\tag{4}$$

$$\mathcal{V}=\mathrm{diag}(1/v_1,1/v_2,\dots,1/v_G),\qquad \mathcal{R}^p=\begin{pmatrix}\chi_1^p&\chi_2^p&\dots&\chi_G^p\end{pmatrix}^T,\tag{5}$$

$$\mathcal{R}_k^d=\begin{pmatrix}\chi_{k,1}^d&\chi_{k,2}^d&\dots&\chi_{k,G}^d\end{pmatrix}^T,\tag{6}$$

The magnitude $\boldsymbol{\Phi}_g^n=\boldsymbol{\Phi}_g^n(x,t)$ denotes the nth-moment of the neutron flux in the spherical harmonics expansion. C_k denotes the delayed neutron precursor concentration. Subindex g ($g=1,\dots,G$) refers to the energy group. Subindex k ($k=1,\dots,K$) refers to the neutron precursors group, where usually the total number K is 6 or 8. The total and the fission macroscopic cross-sections are denoted by Σ_{tg} and Σ_{fg}, respectively. The value of $\Sigma_{sgg'}^n$ is the nth-component of the scattering cross-section in the spherical harmonics expansion. The value of ν_g is the mean number of neutrons produced by fission. The value of v_g denotes the neutron velocity. The spectrum of the prompt and the delayed neutrons are denoted by χ_g^p and $\chi_{g,k}^d$. The fraction of the delayed neutrons is β_k such that the total delayed neutron fraction $\beta=\sum_k^K\beta_k$. Finally, the neutron precursor delayed constants are represented by λ_k. Usually, it is assumed that the scattering is isotropic, therefore $\Sigma_{s,gg'}^n=0$, for $n>1$.

The P_N equations constitute a set of $N+1$ equations with $N+2$ unknowns. The most common option to solve this problem it to remove the term $\nabla\boldsymbol{\Phi}^{N+1}$ that appears in the Nth equation. Other possible solutions, known as closures, have also been studied in the literature (Hauck and McClarren, 2010).

Following the previous notation, the steady-state multigroup SP_N equations are expressed as

$$\nabla\left(\frac{n}{2n+1}\phi^{n-1}+\frac{n+1}{2n+1}\phi^{n+1}\right)+\Sigma^{n,0}\phi^n=\frac{\delta_{n0}}{k_{\mathrm{eff}}}\mathcal{R}\mathcal{F}^0\phi^0\quad n=0,1,\dots,N,\tag{7}$$

where $\phi^n=\boldsymbol{\Phi}^n(x,0)$ is the steady-state flux and

$$\mathcal{R}=\begin{pmatrix}\chi_1&\chi_2&\dots&\chi_G\end{pmatrix}^T,\tag{8}$$

where χ_g is defined as $\chi_g=\chi_g^p(1-\beta)+\sum_k^K\chi_g^{d,k}\beta_k$. Superindex 0 in $\Sigma^{n,0}$ and $\mathcal{F}^0$ indicates that the operators correspond to the value of them in the steady state configuration. k_{eff} is k-effective of the system. The fission cross-sections are divided by k_{eff} when the steady-state problem is solved to assume that the reactor is in a critical state. Therefore, in the following, it is supposed that $k_{\mathrm{eff}}=1$.

To develop the neutron noise equations, the quantities are split into the sum of the mean and the oscillatory part as

$$\begin{aligned}&\boldsymbol{\Phi}^n=\phi^n+\delta\boldsymbol{\Phi}^n,\qquad &&\Sigma^n=\Sigma^{n,0}+\delta\Sigma^n,\\&\mathcal{F}=\mathcal{F}^0+\delta\mathcal{F},\qquad &&C_k=C_k^0+\delta C_k,\end{aligned}\tag{9}$$

where for all the quantities p is assumed that $\langle\delta p\rangle=0$ which result in $\langle p\rangle=p^0$ i.e. the processes are assumed stationary and $\|\delta p\|\ll\|p^0\|$, i.e. the fluctuations are much smaller than the magnitudes in steady-state. Also, It must be reminded that neutron noise equations are not defined at $\omega=0$ if the mean value of the perturbed term (noise source) is not zero.

Substituting the neutron noise separations (9) into the Eqs. (1) and (2), using the steady-state equations (7) and removing the second order terms, we obtain the first-order neutron noise FSP_N equations

$$\begin{aligned}&\mathcal{V}\frac{\partial}{\partial t}\delta\boldsymbol{\Phi}^n+\nabla\left(\frac{n}{2n+1}\delta\boldsymbol{\Phi}^{n-1}+\frac{n+1}{2n+1}\delta\boldsymbol{\Phi}^{n+1}\right)+\Sigma^{n,0}\delta\boldsymbol{\Phi}^n+\delta\Sigma^n\phi^n\\&=\delta_{n,0}\left((1-\beta)\mathcal{R}^p\left(\mathcal{F}^0\delta\boldsymbol{\Phi}^0+\delta\mathcal{F}\phi^0\right)+\sum_{k=1}^{K}\lambda_k\mathcal{R}_k^d\delta C_k\right),\quad n=0,1,\dots,N,\end{aligned}\tag{10}$$

where the equations for the neutron precursors are

$$\frac{\partial}{\partial t}\delta C_k=-\lambda_k\delta C_k+\beta_k\left(\mathcal{F}^0\delta\boldsymbol{\Phi}^0+\delta\mathcal{F}\phi^0\right),\qquad k=1,\dots,K.\tag{11}$$

Fig. 1. One-dimensional problem.

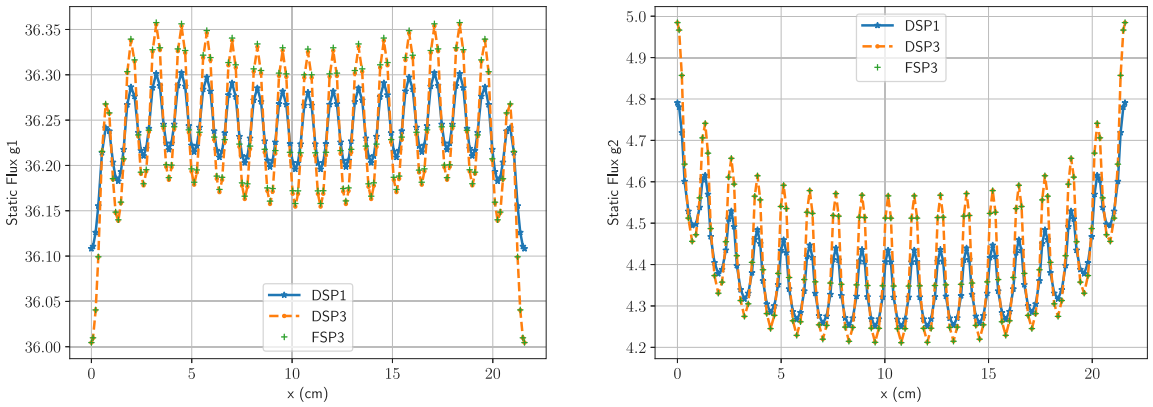

(a) Fast Flux (b) Thermal Flux

Fig. 2. Steady-state solution in the one-dimensional benchmark.

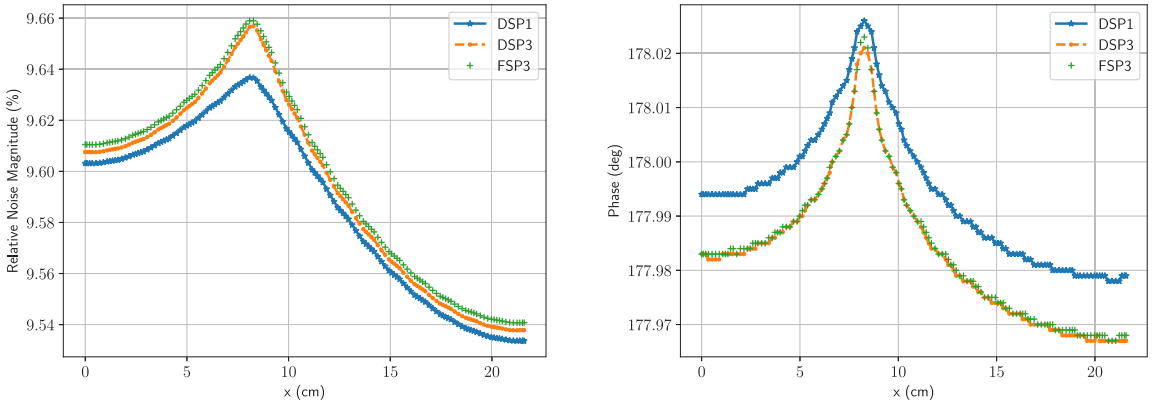

(a) Fast Flux Noise Amplitude (%) (b) Thermal Flux Noise Amplitude (%)

Fig. 3. Relative noise amplitude in the one-dimensional benchmark.

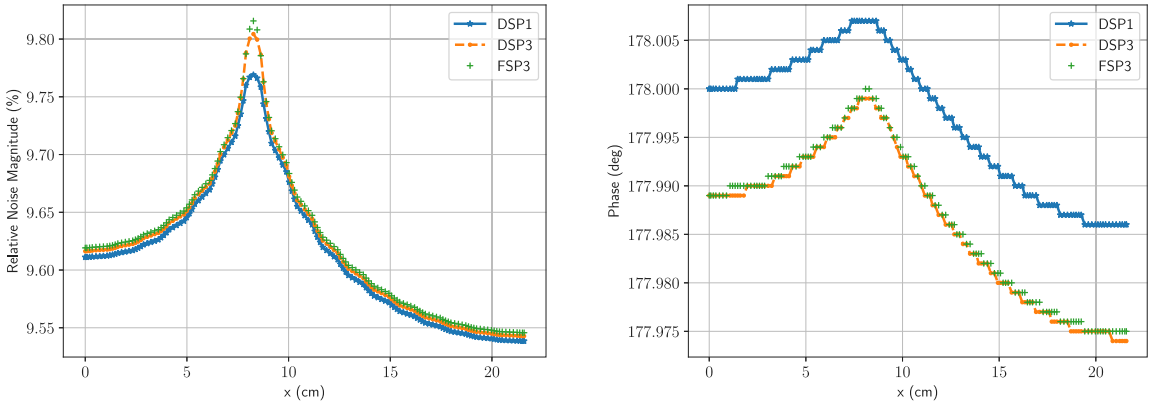

(a) Fast Flux Noise Phase (b) Thermal Flux Noise Phase

Fig. 4. Noise phase in the one-dimensional benchmark.

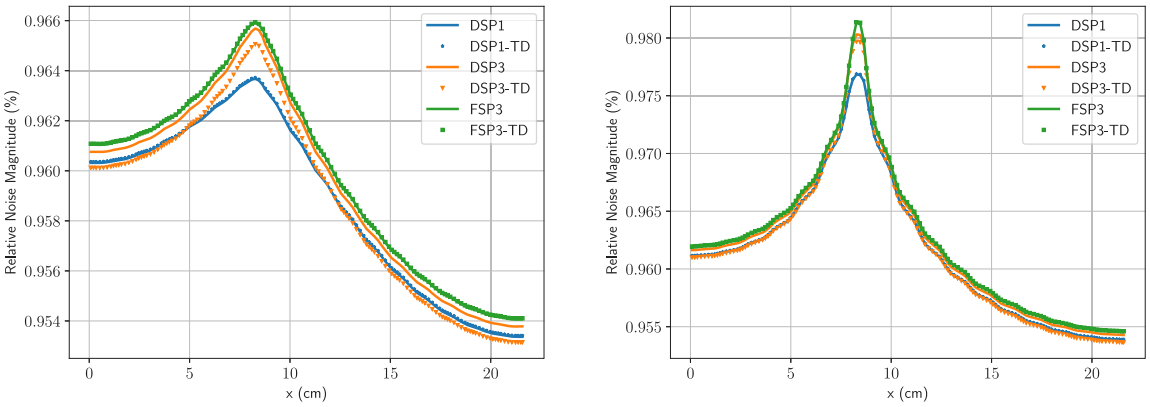

(a) Fast Flux Noise Amplitude (b) Thermal Flux Noise Amplitude

Fig. 5. Relative noise amplitudes in time-domain and frequency-domain calculations in the one-dimensional benchmark.

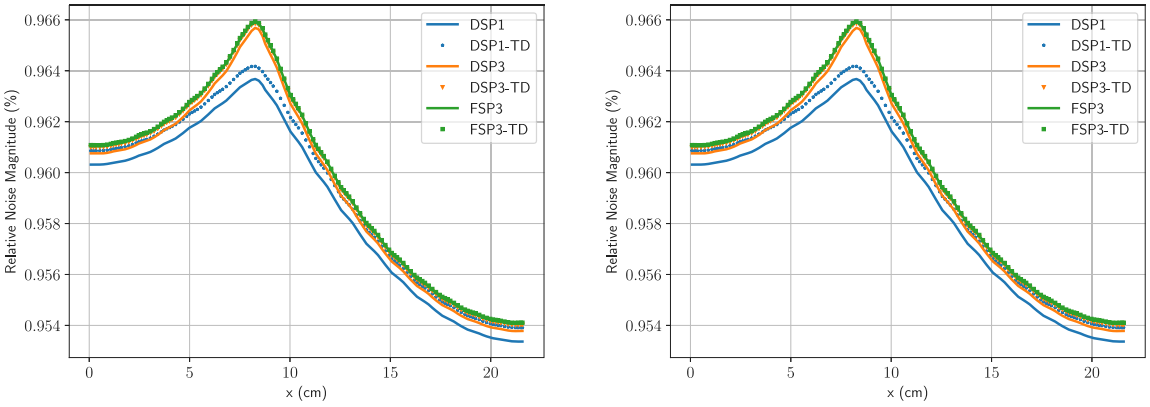

(a) Fast Flux Noise Amplitude (b) Thermal Flux Noise Amplitude

Fig. 6. Relative noise amplitudes in time-domain and frequency-domain calculations in the one-dimensional benchmark not considering $\delta\Sigma_{tr} \approx 0$ in time-domain calculations.

To obtain the neutron noise equations in the frequency domain, the following step is to apply the Fourier Transform, defined as,

$$f(\omega) = \mathcal{F}[f(t)] = \int_{-\infty}^{\infty} \exp(-i\omega t) f(t) dt, \tag{12}$$

to the previous equations, which permits isolating the concentration of precursors from Eq. (11) and substitute this term into Eq. (10). The frequency-domain equation, once the precursors' term is removed, has the form

$$\begin{aligned} &i\omega \mathcal{V}\delta\boldsymbol{\Phi}_g^n + \nabla\left(\frac{n}{2n+1}\delta\boldsymbol{\Phi}^{n-1} + \frac{n+1}{2n+1}\delta\boldsymbol{\Phi}^{n+1}\right) + \Sigma^{n,0}\delta\boldsymbol{\Phi}^n \\ &- \delta_{n,0}\Gamma\mathcal{F}^0\delta\boldsymbol{\Phi}^0 = -\delta\Sigma^n\phi^n + \delta_{n,0}\Gamma\delta\mathcal{F}\phi^0, \quad n = 0, 1, \ldots, N, \end{aligned} \tag{13}$$

where

$$\Gamma = (1-\beta)\mathcal{R}^p + \sum_{k=1}^{K} \frac{\lambda_k\beta_k}{i\omega + \lambda_k}\mathcal{R}_k^d. \tag{14}$$

3. Neutron noise in the diffusive SP_N approximation (DSP_N)

An alternative time-formulation of the SP_N approximation can be considered if the time derivatives of the odd moments are assumed to be null, i.e.

$$\frac{\partial\boldsymbol{\Phi}^n}{\partial t} = 0, \qquad n \text{ odd}. \tag{15}$$

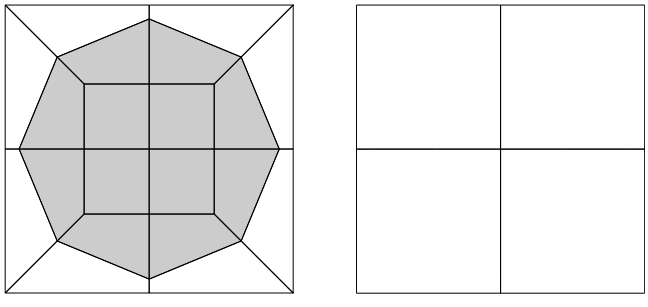

Fig. 7. Spatial discretization of each pin cell (left) and reflector cell (right).

This consideration permits substituting the equations related to the odd moments into the equations of the even moments to obtain a simpler formulation where only the even moments are involved. This approximation is known as diffusive SP_N equations (Carreño et al., 2021) (DSP_N equations).

To develop the neutron noise equations associated with this model, we start with the time-domain DSP_N equations (DSP_N-TD equations)

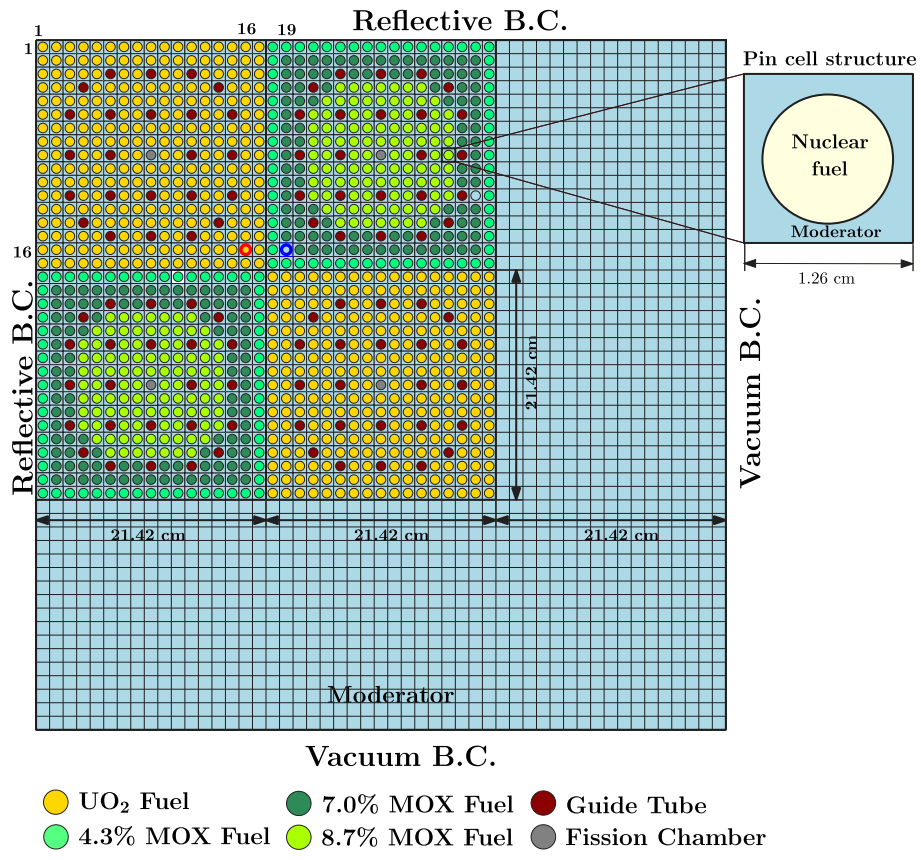

Fig. 8. Definition of 2D C5G7 benchmark. The perturbed pin in marked with a red circle.

where all moments appear in the equations

$$\begin{aligned}
&\mathcal{V}\frac{\partial}{\partial t}\boldsymbol{\Phi}^n + \nabla\left(\frac{n}{2n+1}\boldsymbol{\Phi}^{n-1} + \frac{n+1}{2n+1}\boldsymbol{\Phi}^{n+1}\right) + \Sigma^n\boldsymbol{\Phi}^n \\
&\qquad = \delta_{n,0}\Big((1-\beta)\mathcal{R}^p\mathcal{F}\boldsymbol{\Phi}^0 + \sum_{k=1}^{K}\lambda_k\mathcal{R}_k^d C_k\Big), \qquad n \text{ even}, \\
&\nabla\left(\frac{n}{2n+1}\boldsymbol{\Phi}^{n-1} + \frac{n+1}{2n+1}\boldsymbol{\Phi}^{n+1}\right) + \Sigma^n\boldsymbol{\Phi}^n = 0, \qquad n \text{ odd},
\end{aligned} \tag{16}$$

and the evolution of the delayed neutron precursor concentration is given by Eq. (2). The steady-state equations associated with the DSP_N equations are the same as the ones of the full formulation, which are given by Eq. (7). Moreover, the decomposition considered in Eq. (9) is also taken into account, to get the first order neutron noise diffusive SP_N equations

$$\begin{aligned}
&\mathcal{V}\frac{\partial}{\partial t}\delta\boldsymbol{\Phi}^n + \nabla\left(\frac{n}{2n+1}\delta\boldsymbol{\Phi}^{n-1} + \frac{n+1}{2n+1}\delta\boldsymbol{\Phi}^{n+1}\right) + \Sigma^{n,0}\delta\boldsymbol{\Phi}^n + \delta\Sigma^n\phi^n \\
&\qquad = \delta_{n,0}\left((1-\beta)\mathcal{R}^p(\mathcal{F}^0\delta\boldsymbol{\Phi}^0 + \delta\mathcal{F}\phi^0) + \sum_{k=1}^{K}\lambda_k\mathcal{R}_k^d\delta C_k\right), \qquad n \text{ even}, \\
&\nabla\left(\frac{n}{2n+1}\delta\boldsymbol{\Phi}^{n-1} + \frac{n+1}{2n+1}\delta\boldsymbol{\Phi}^{n+1}\right) + \Sigma^{n,0}\delta\boldsymbol{\Phi}^n + \delta\Sigma^n\phi^n = 0, \qquad n \text{ odd},
\end{aligned} \tag{17}$$

where the precursors are given by Eq. (11).

If now the Fourier transform is applied to Eq. (17) and a similar process as the one used for the FSP_N formulation is done, the following equations are obtained,

$$\begin{aligned}
&i\omega\mathcal{V}\delta\boldsymbol{\Phi}^n + \nabla\left(\frac{n}{2n+1}\delta\boldsymbol{\Phi}^{n-1} + \frac{n+1}{2n+1}\delta\boldsymbol{\Phi}^{n+1}\right) + \Sigma^{n,0}\delta\boldsymbol{\Phi}^n + \delta\Sigma^n\phi^n \\
&\qquad = \delta_{n,0}\left(\left((1-\beta)\mathcal{R}^p + \sum_{k=1}^{K}\frac{\lambda_k\beta_k}{i\omega+\lambda_k}\mathcal{R}_k^d\right)\left(\mathcal{F}^0\delta\boldsymbol{\Phi}^0 + \delta\mathcal{F}\phi^0\right)\right), \qquad n \text{ even},
\end{aligned} \tag{18}$$

$$\nabla\left(\frac{n}{2n+1}\delta\boldsymbol{\Phi}^{n-1} + \frac{n+1}{2n+1}\delta\boldsymbol{\Phi}^{n+1}\right) + \Sigma^{n,0}\delta\boldsymbol{\Phi}^n + \delta\Sigma^n\phi^n = 0, \qquad n \text{ odd}. \tag{19}$$

This diffusive formulation of the SP_N equations permits isolating the odd moments from their associated Eqs. (19) and to substitute them into the equation for even moments (18). Moreover, we assume that $\nabla\frac{\delta\Sigma^n}{(\Sigma^{n,0})^2} = 0$, for n even. In neutron noise diffusion approximation (Larsson and Demazière, 2009; Demaziere, 2011) and diffusive SP_3 equations (Gong et al., 2021), it is assumed that the fluctuations in generalized diffusive coefficients i.e. $\delta D_n = 0$. These assumptions imply that the term of Eq. (19) $\nabla\frac{\delta\Sigma^n}{(\Sigma^{n,0})^2} = 0$ for n even.

Then, the DSP_N-FD equations are:

$$\begin{aligned}
&i\omega\mathcal{V}\delta\boldsymbol{\Phi}^n - \nabla\left[\frac{n(\Sigma^{n-1,0})^{-1}}{(2n+1)(2n-1)}\nabla\left((n-1)\delta\boldsymbol{\Phi}^{n-2} + n\delta\boldsymbol{\Phi}^n\right)\right. \\
&\left. + \frac{(n+1)(\Sigma^{n+1,0})^{-1}}{(2n+1)(2n+3)}\nabla\left((n+1)\delta\boldsymbol{\Phi}^n + (n+2)\delta\boldsymbol{\Phi}^{n+2}\right)\right] \\
&+ \Sigma^{n,0}\delta\boldsymbol{\Phi}^n - \delta_{n,0}\Gamma\mathcal{F}^0\delta\boldsymbol{\Phi}^0 = -\delta\Sigma^n\phi^n + \delta_{n,0}\Gamma\delta\mathcal{F}\phi^0, \qquad n=0,2,\ldots,N-1,
\end{aligned} \tag{20}$$

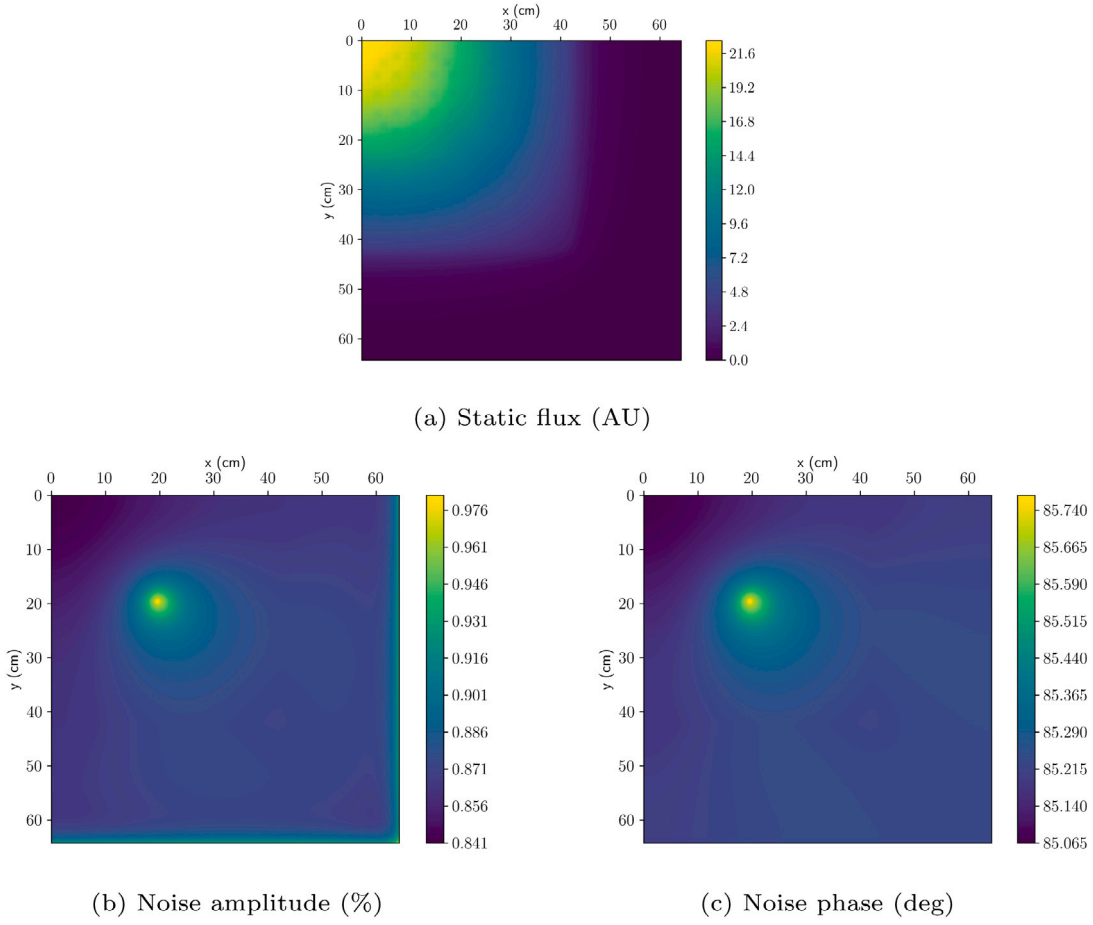

(a) Static flux (AU)

(b) Noise amplitude (%)

(c) Noise phase (deg)

Fig. 9. Results associated with the 1st energy group in the 2D C5G7 NN1.1 case.

where

$$\Gamma = (1-\beta)\mathcal{R}^p + \sum_{k=1}^{K} \frac{\lambda_k \beta_k}{i\omega + \lambda_k} \mathcal{R}_k^d. \tag{21}$$

Note that if $N = 1$ this approximation is equivalent to the neutron noise diffusion equation. And, it coincides with the one presented in Demaziere (2011) when $g = 2$ are considered.

For instance, for $N = 3$, the DSP$_3$-FD equations are

$$\begin{aligned} i\omega\mathcal{V}\delta\boldsymbol{\Phi}^0 - \nabla\frac{(\Sigma^{1,0})^{-1}}{3}\nabla\left(\delta\boldsymbol{\Phi}^0 + 2\delta\boldsymbol{\Phi}^2\right) + \Sigma^{0,0}\delta\boldsymbol{\Phi}^0 - \Gamma\mathcal{F}^0\delta\boldsymbol{\Phi}^0 \\ = -\delta\Sigma^0\phi^0 + \Gamma\delta\mathcal{F}\phi^0, \\ i\omega\mathcal{V}\delta\boldsymbol{\Phi}^2 - \nabla\left[\frac{2(\Sigma^{1,0})^{-1}}{15}\nabla\left(\delta\boldsymbol{\Phi}^0 + 2\delta\boldsymbol{\Phi}^2\right)\right. \\ \left. + \frac{9(\Sigma^{3,0})^{-1}}{35}\nabla\delta\boldsymbol{\Phi}^2\right] + \Sigma^{2,0}\delta\boldsymbol{\Phi}^2 = -\delta\Sigma^2\phi^2, \end{aligned} \tag{22}$$

For this formulation, we apply a linear transformation of the variables similar to the one applied in Hamilton and Evans (2015) to have only one unknown with the gradients. The new variables are defined as

$$W^1 = \delta\phi^0 + 2\delta\phi^2, \qquad \delta W^2 = 3\delta\phi^2, \tag{23}$$

$$\delta U^1 = \delta\boldsymbol{\Phi}^0 + 2\delta\boldsymbol{\Phi}^2, \qquad \delta U^2 = 3\delta\boldsymbol{\Phi}^2. \tag{24}$$

Eq. (22) with this change of variables gives a problem of the form

$$(\mathbb{V} - \nabla\mathbb{D}\nabla + \mathbb{S} + \mathbb{F})\delta U = -(\delta\mathbb{S} + \delta\mathbb{F})W, \tag{25}$$

where

$$\delta U = (\delta U^1, \delta U^2), \qquad W = (W^1, W^2), \tag{26}$$

$$\bar{\mathbb{V}}_{ab} = \sum_{m=1}^{2} \bar{c}_{ab}^{(m)} i\omega\mathcal{V}, \qquad \bar{\mathbb{D}} = \begin{pmatrix} \frac{1}{3}(\Sigma^{1,0})^{-1} & 0 \\ 0 & \frac{3}{35}(\Sigma^{3,0})^{-1} \end{pmatrix}, \tag{27}$$

$$\bar{\mathbb{S}}_{ab} = \sum_{m=1}^{2} \bar{c}_{ab}^{(m)} \Sigma^{m,0}, \qquad \bar{\mathbb{F}}_{ab} = \bar{c}_{ab}^{(1)} \Gamma\mathcal{F}^0, \tag{28}$$

$$\delta\bar{\mathbb{S}}_{ab} = \sum_{m=1}^{2} \bar{c}_{ab}^{(m)} \delta\Sigma^m, \qquad \delta\bar{\mathbb{F}}_{ab} = \bar{c}_{ab}^{(1)} \Gamma\delta\mathcal{F}, \tag{29}$$

and the coefficients matrices, $\bar{c}^{(m)}$, are

$$\bar{c}^{(1)} = \begin{pmatrix} 1 & -2/3 \\ -2/5 & 4/15 \end{pmatrix}, \qquad \bar{c}^{(2)} = \begin{pmatrix} 0 & 0 \\ 0 & 1/3 \end{pmatrix}.$$

4. Numerical results

The differential full and diffusive SP$_N$ equations (FSP$_N$ and DSP$_N$) in frequency-domain are spatially discretized by using a continuous Galerkin finite element method with Lagrange polynomials of order 3. This discretization is implemented in C++ by using structures from the open-source libraries `deal.II` (Bangerth et al., 2007) and library PETSc (Balay et al., 2015). This part has been developed as an extension of the open source neutronic code `FEMFFUSION` (Vidal-Ferràndiz et al., 2020b). More details about the implementation of the time-dependent SP$_3$ equations with the finite element method are found in Carreño et al. (2021).

From the spatial discretization of the differential frequency-domain formulations, an algebraic system of linear equations with complex

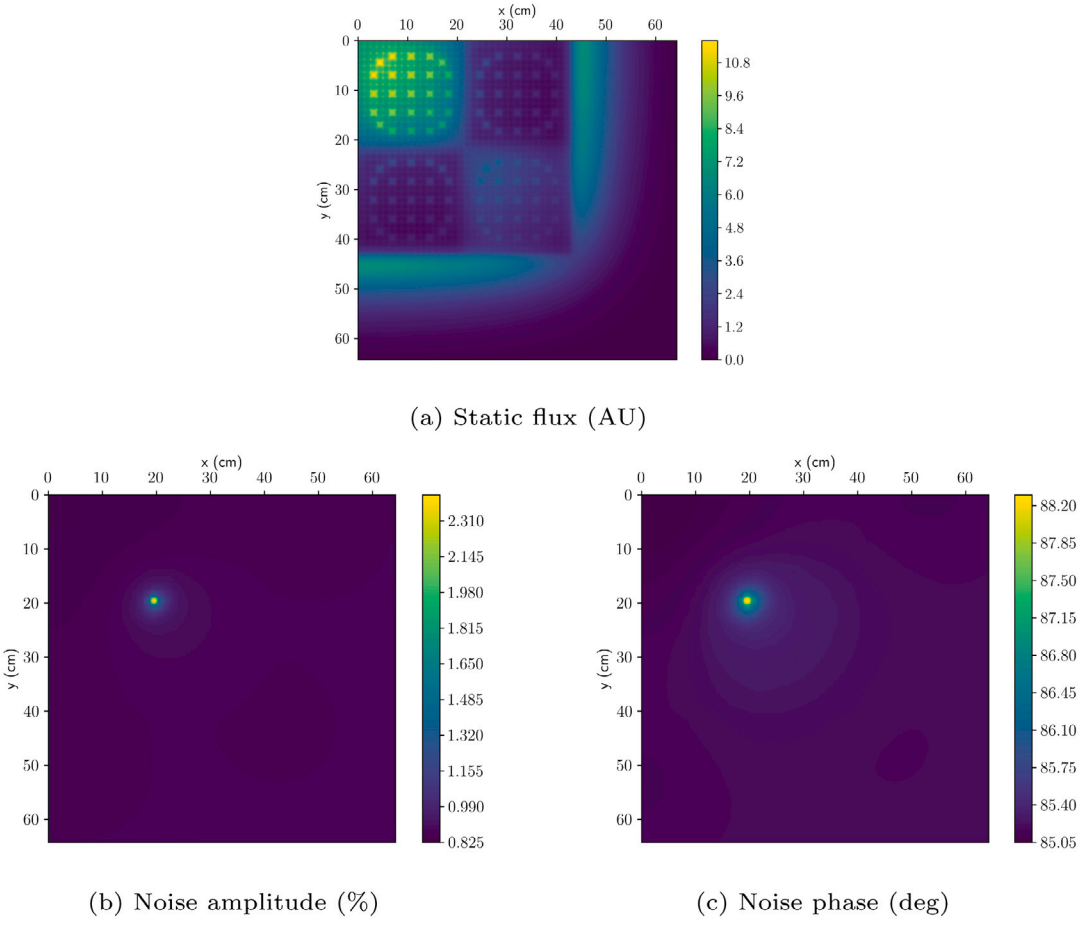

Fig. 10. Results associated with the 7th energy group in the 2D C5G7 NN1.1 case.

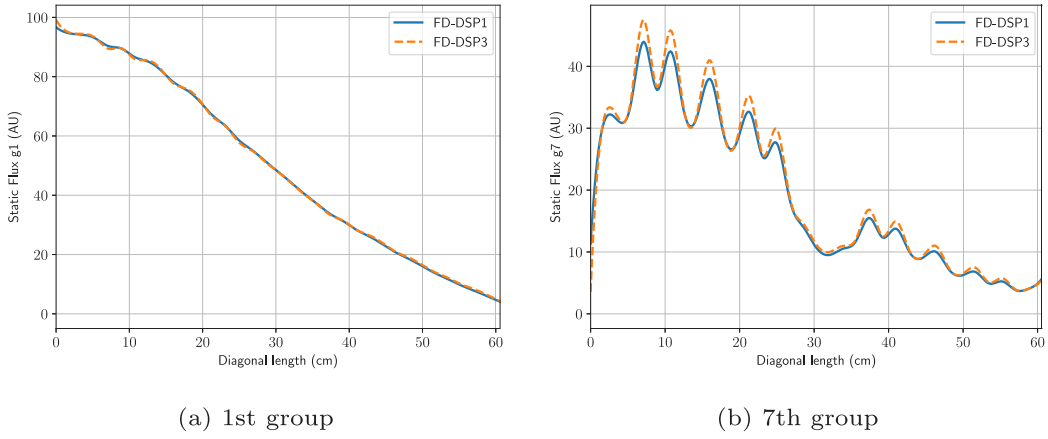

Fig. 11. Static scalar flux along the main diagonal of the 2D C5G7 case.

coefficients is obtained. To solve this system, we have used the GMRES method with the ILU preconditioner provided by PETSc library for complex numbers (Balay et al., 2015). Alternatively, one can transform the complex system into a real-number system and then apply the ILU preconditioner and the GMRES solver. However, in the problems presented in numerical results, the classical transformations do not improve the convergence of the linear system solver. Further studies are needed to design preconditioners to improve the convergence of these systems in complex and real arithmetic.

To compare the performance of the two SP_N formulations presented in the frequency-domain, two benchmark problems will be analysed, a one-dimensional problem and the C5G7 neutron noise benchmark.

4.1. One-dimensional problem

To test the frequency-domain SP_N equations proposed with both formulations, we solve a one-dimensional benchmark composed by 17 homogeneous square fuel pins of length 1.26 cm as Fig. 1 shows. This

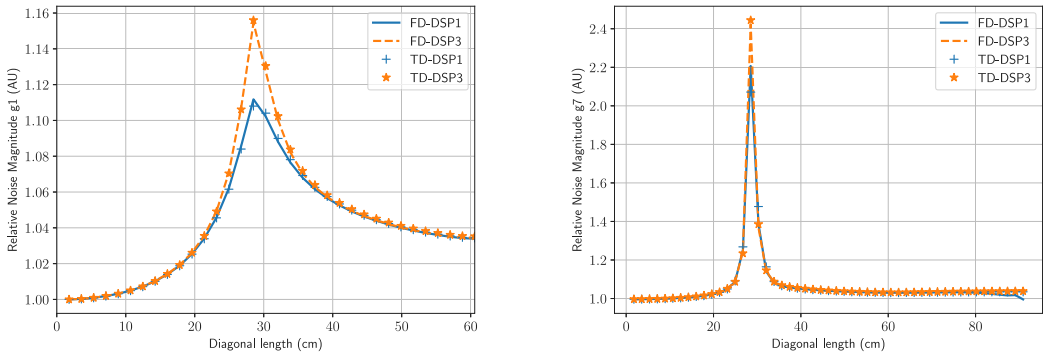

(a) 1st group noise amplitude (%) (b) 7th group noise amplitude (%)

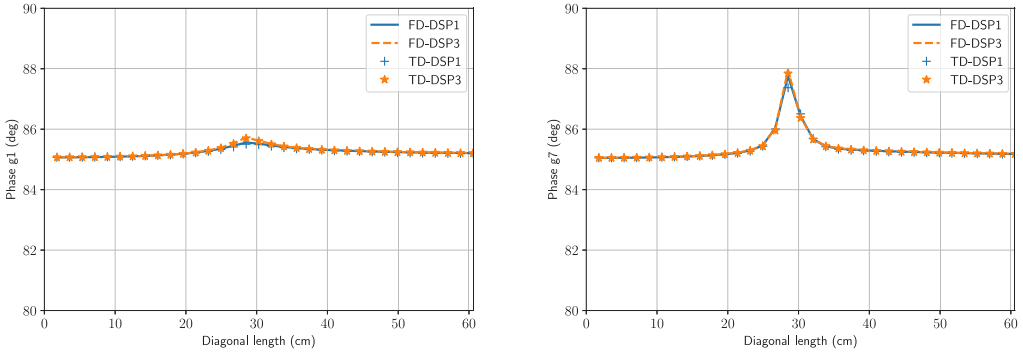

(c) 1st group noise phase (deg) (d) 7th group noise phase (deg)

Fig. 12. Noise amplitude and phase along the main diagonal of the 2D C5G7 NN1.1 case.

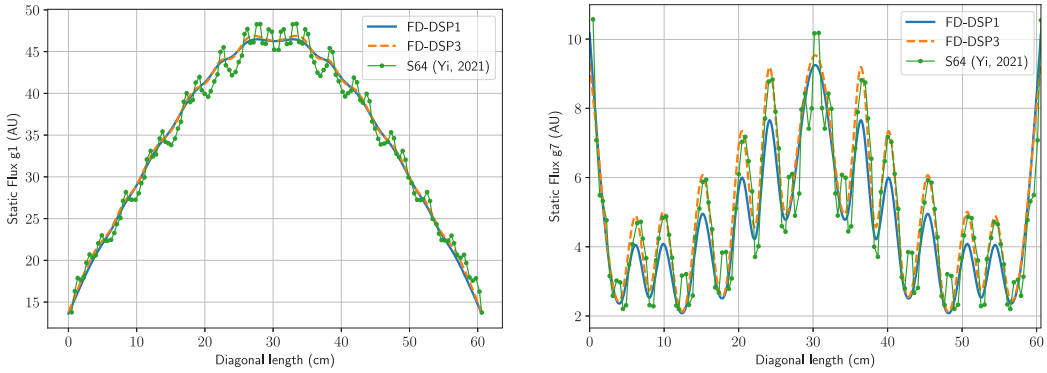

(a) 1st group (b) 7th group

Fig. 13. Static scalar flux along the diagonal that crosses the MOX fuel assemblies of the 2D C5G7 reactor.

problem is a one-dimensional version of the case 2 solved in Vinai et al. (2021a). Each fuel pin is divided into 8 cells: 4 cells of length 0.13215 cm to model the moderator and 4 cells of length 0.18285 cm to model the fuel. Two extra cells of moderator of 0.08 cm are added at the edges of the problem. The cross sections used are defined in Table 1. Zero current is used for the boundary conditions. A perturbation located in the seventh fuel pin (marked in green) is introduced at $t = 0$, as a sinusoidal variation of the cross sections of the form:

$$\delta\Sigma_t(t) = 0.004\ \Sigma_t^0 \sin\left(\omega_0 t\right),$$
$$\delta\Sigma_s(t) = 0.0034\ \Sigma_s^0 \sin\left(\omega_0 t\right),$$
$$\delta\Sigma_f(t) = 0.002\ \Sigma_f^0 \sin\left(\omega_0 t\right).$$

The angular frequency of the perturbation is set to $\omega_0 = 2\pi$, in other words, a frequency of 1 Hz. This type of perturbation over the macroscopic cross-sections is a generic one, and other types of perturbations as mechanical oscillations or density fluctuations of the coolant flow can be expressed as linear combinations of perturbations of this kind.

Fig. 2 shows the results for the amplitudes associated with the static scalar fluxes and the phases obtained with the diffusive SP_1 (DSP_1), the Diffusive SP_3 approximation (DSP_3) and the Full SP_3 approximation (FSP_3). We have to take into account that the steady-state FSP_3 and DSP_3 formulations are mathematically equivalent. SP_3 approximations represent more accurately the neutron flux, specially when there is a strong change in the gradient of the neutron flux. This difference can be seen in the peaks in the centre of the water blades and the fuel pins.

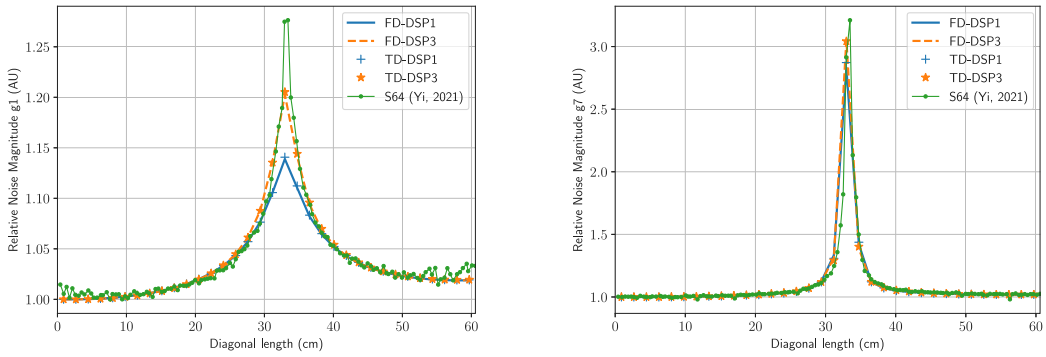

(a) 1st group noise amplitude (%) (b) 7th group noise amplitude (%)

Fig. 14. Noise amplitude along the diagonal that crosses the MOX fuel assemblies of the 2D C5G7 NN1.2 case.

Table 1
Nuclear data for the one-dimensional benchmark.

Data	Fuel	Moderator
Σ_{t1} (cm^{-1})	0.37790	0.25411
Σ_{t2} (cm^{-1})	0.55064	1.2182
Σ_{a1} (cm^{-1})	0.025755	0.00079457
Σ_{a2} (cm^{-1})	0.15788	0.02931600
Σ_{f1} (cm^{-1})	0.0057671	0.00
Σ_{f2} (cm^{-1})	0.1062200	0.00
ν_1 (–)	2.59068	0.00
ν_2 (–)	2.59068	0.00
Σ_{12} (cm^{-1})	0.0008647	0.028124
$\mathbf{v}_1$ (cm s^{-1})	$1.823\,04 \times 10^7$	
$\mathbf{v}_2$ (cm s^{-1})	$4.130\,67 \times 10^5$	
β_{eff} (–)	0.0535	
Λ (s^{-1})	0.0851	

Table 2
Relative maximum difference (RMD) and relative average difference (RAD) with respect to FSP_3 in the one-dimensional benchmark.

	Fast Group		Thermal Group	
	RMD (%)	RAD (%)	RMD (%)	RAD (%)
DSP_1	0.231	0.103	0.475	0.098
DSP_3	0.034	0.031	0.115	0.029

Fig. 3 shows the relative neutron noise amplitude (%) and Fig. 4 shows the neutron noise phase in the one-dimensional benchmark for DSP_1, DSP_3 and FSP_3. The relative maximum difference (RMD) and the relative average difference (RAD) between DSP_1 and DSP_3 with respect to FSP_3 are shown in Table 2. On the one hand, an improvement over the DSP_1 approximation can be seen for DSP_3 and FSP_3 formulations. On the other hand, FSP_3 does not show remarkable difference with respect to its diffusive approximation, DSP_3. The maximum differences are located around the perturbed cell. It must be noted that in a one-dimensional case, the FSP_3 linear system is twice bigger than the DSP_3 system, and its associated matrix is worse conditioned (Carreño et al., 2019). Due to the difficulties to solve the FSP_3 approximation and the no significant differences found with respect the DSP_3, the full formulation is not further considered . Similar results can be observed for the neutron noise phase. However, the global change in the phase is less than 1 degree.

To validate the results shown, time-domain calculations are performed using the same approximations. To obtain accurate results in the time-domain, 3 complete periods of the perturbation are considered, and the time-step for the time integration method is set to 0.01 s. Fig. 5 displays time-domain (TD) alongside frequency-domain (FD) calculations for the neutron noise magnitude with the same conditions. Time-domain results have been transformed to the frequency-domain by applying the Fast Fourier Transform (FFT) and only the results for 1 Hz are shown. Other frequencies, different from the perturbation's frequency, show a negligible noise amplitude (Vidal-Ferràndiz et al., 2020a). An almost perfect match between both methodologies can be observed. However, time-domain calculation are 5 to 50 times slower because they must solve a real-valued linear system for each time step, and in this problem we need to solve 300 linear systems.

Despite the close agreement between time-domain and frequency-domain calculations observed in Fig. 5, it is possible to improve SP_1-TD and SP_3-TD results by not including the approximation of $\delta\Sigma_t = 0$. These results are shown in Fig. 6. It must be noted that FSP_N-FD calculation does use this approximation. This Figure shows a little difference in the DSP_1 results if the term $\delta\Sigma_{tr} \neq 0$ is introduced in the equations.

4.2. C5G7 neutron noise benchmark

To compare the equations in a more realistic nuclear system, two neutron noise problems from the 2D-C5G7 benchmark (Lewis et al., 2001) are used. These problems correspond to the NN1.1 and NN1.2 cases defined in Vinai et al. (2019).

The configuration of this reactor consists of a core with 2 MOX and 2 UO_2 square fuel assemblies surrounded by a moderator region, as it is shown in Fig. 8. Each fuel assembly consists of 17 × 17 square fuel pin cells of size 1.26 × 1.26 cm^2. Each pin cell is made of a circular fuel, guide tube or fission chamber region of radius 0.54 cm surrounded by moderator. This benchmark is defined with seven energy group cross-sections for each material. The kinetic parameters and the data for eight groups of delayed neutron precursors are given in Boyarinov et al. (2016).

Both neutron noise cases studied in this work are defined by the perturbation of the capture cross-sections. The NN1.1 problem perturbs the fuel pin located at (16,16) in the UO_2 assembly (marked with a red circle in Fig. 8) and NN1.2 case sets the perturbations in the fuel pin at position (16,19) within the MOX fuel assembly (marked with a blue circle in Fig. 8).

The perturbations in the capture cross-section are given by

$$\delta\Sigma_{cg}(t) = 0.05\ \Sigma^0_{cg}\ \sin(2\pi t)\,, \qquad g = 1, \ldots, G\,. \tag{30}$$

This oscillation of the capture cross-section produces fluctuations of the absorption and total cross-sections as,

$$\delta\Sigma_{ag}(t) = 0.05\ \Sigma^0_{cg}\ \sin(2\pi t)\,, \qquad g = 1, \ldots, G\,, \tag{31}$$

$$\delta\Sigma_{tg}(t) = 0.05\ \Sigma^0_{cg}\ \sin(2\pi t)\,, \qquad g = 1, \ldots, G\,, \tag{32}$$

where capture cross-section is calculated as $\Sigma^0_{cg} = \Sigma^0_{ag} - \Sigma^0_{fg}$.

The grid shown in Fig. 7 is used to make the spatial discretization of pin cells, because its application provides accurate results in the steady-state problem (Vidal-Ferràndiz et al., 2019b). The area in grey in the

grid is equal to the area of the circle of the pin. The total number of cells in the grid is 28900. Second degree polynomials are used in the finite element method, so a problem of 1624126 degrees of freedom in the DSP3 case is obtained.

In the following, only the diffusive SP_N equations are considered (DSP_N). First, the NN1.1 case is analysed. Figs. 9 and 10 display the steady-state, relative noise amplitude and noise phase of the 1st and 7th energy group in this case, respectively. These results have been computed with the DSP_3 equations in the frequency-domain.

Now, the NN1.1 results of the DSP_1 and DSP_3 equations in frequency-domain (DSP_1-FD and DSP_3-FD) are compared with the results in the time-domain (DSP_1-TD and DSP_3-TD) along the main diagonal. Frequency-domain computations assume that $\delta\Sigma_t \approx 0$, while time-domain computations do not use this approximation. Fig. 11 plots the steady-state scalar fluxes for the 1st and 7th energy group along the main diagonal of the 2D C5G7 reactor. This Figure shows that relevant differences can be observed for the thermal group. Fig. 12 displays the amplitudes and phases of the neutron noise for the 1st and the 7th energy group along the main diagonal. Figures of the amplitudes show differences between the FD and TD less than 0.8% for all approximations. However, the peak in the perturbed cell in the DSP_3 results, where the gradient of the neutron noise is larger, is stronger than for the DSP_1 approximation. The maximum difference between DSP_1 and DSP_3 is about 4.3% for the 1st energy group and 10.4% for the 7th energy group. This improvement only makes the computation approximately twice as demanding in terms of memory and computational time. Difference in the neutron noise phase between the 4 methodologies are negligible in absolute terms, less than 0.06 degrees, and they are probably due to the numerical tolerances used in the iterative solvers, spatial discretization errors and the numerical Fourier Transform performed.

Second, NN1.2 results for both the frequency-domain equations (DSP_1-FD and DSP_3-FD) and the time-domain equations (DSP_1-TD and DSP_3-TD) are compared with a frequency-domain discrete ordinates reference using S_{64} extracted from Yi et al. (2021). Fig. 13 shows the static scalar flux obtained with these approximations. This Figure shows that S_{64} represents more accurately the strong changes in the gradients of the neutron flux, but DSP_1 and DSP_3 approximations accurately represent the average values of the steady state neutron flux. Fig. 14 compares the amplitudes of the neutron noise for the 1st and the 7th energy group along the diagonal that crosses the MOX fuel assemblies of the 2D-C5G7 reactor. This Figure verifies that the DSP_3 equations solves more accurately the neutron noise problem in comparison with DSP_1 approximation. For the fast energy group, the maximum difference between S_{64} and DSP_3 is less than 6.2% while this difference is about 10.1% against the DSP_1. For the thermal group, the maximum difference between S_{64} and DSP_3 is 16.0% and against the DSP_1 is 28.3%.

5. Conclusions

This work presents the frequency-domain SP_N equations for the diffusive and the full formulation. A comparison between the two types of formulations is provided over two neutron noise problems: a one-dimensional case and a neutron noise problem in the 2D-C5G7 reactor. A continuous finite element method is used for the spatial discretization of the equations.

Numerical results show that frequency-domain equations provide as accurate solutions as the time-domain simulations but, generally, they are faster because only a linear system with complex coefficients must be solved for the frequency-domain equations.

Approximations of order $N = 3$ with the SP_N equations obtain more accurate results than the DSP_1 approximation in neutron noise problems for problems with large gradient in the neutron flux. Between the diffusive and full formulations, the differences are negligible if $\delta\Sigma_t$ is small enough. Therefore, to provide an accurate solution, with reasonable computational demands, the diffusive SP_N (DSP_N) approximation should be applied.

Future works will be devoted to develop the frequency-domain equations for higher approximations of the neutron transport equation (see

Declaration of competing interest

The authors declare that they have no known competing financial interests or personal relationships that could have appeared to influence the work reported in this paper.

Acknowledgements

This work has been partially supported by Spanish Ministerio de Economía *y* Competitividad under projects ENE2017-89029-P and MTM2017-85669-P. Furthermore, this work has been financed by the Generalitat Valenciana under the project PROMETEO/2018/035.

References

Balay, S., Abhyankar, S., Adams, M.F., Brown, J., Brune, P., Buschelman, K., Dalcin, L., Eijkhout, V., Gropp, W.D., Kaushik, D., Knepley, M.G., McInnes, L.C., Rupp, K., Smith, B.F., Zampini, S., Zhang, H., 2015. PETSc Users Manual. Technical Report ANL-95/11 - Revision 3.6, Argonne National Laboratory, URL http://www.mcs.anl.gov/petsc.

Bangerth, W., Hartmann, R., Kanschat, G., 2007. Deal.II –A general-purpose object-oriented finite element library. ACM Trans. Math. Softw. 33 (4), 24. http://dx.doi.org/10.1145/1268776.1268779.

Boyarinov, V., Fomichenko, P., Hou, J., Ivanov, K., Aures, A., Zwermann, W., Velkov, K., 2016. Deterministic time-dependent neutron transport benchmark without spatial homogenization (C5G7-TD). Nuclear Energy Agency Organisation for Economic Co-Operation and Development (NEA-OECD), Paris, France.

Carreño, A., Vidal-Ferràndiz, A., Ginestar, D., Verdú, G., 2019. Modal methods for the neutron diffusion equation using different spatial modes. Prog. Nucl. Energy 115, 181–193. http://dx.doi.org/10.1016/j.pnucene.2019.03.040.

Carreño, A., Vidal-Ferràndiz, A., Ginestar, D., Verdú, G., 2021. Time-dependent simplified spherical harmonics formulations for a nuclear reactor system. Nucl. Eng. Technol. 53 (12), 3861–3878. http://dx.doi.org/10.1016/j.net.2021.06.010.

Chao, Y.-A., 2016. A new and rigorous SP N theory for piecewise homogeneous regions. Ann. Nucl. Energy 96, 112–125. http://dx.doi.org/10.1016/j.anucene.2016.06.010.

Demaziere, C., 2011. CORE SIM: A multi-purpose neutronic tool for research and education. Ann. Nucl. Energy 38 (12), 2698–2718. http://dx.doi.org/10.1016/j.anucene.2011.06.010.

Demazière, C., 2019. Modelling of Nuclear Reactor Multi-Physics: From Local Balance Equations to Macroscopic Models in Neutronics and Thermal-Hydraulics. Academic Press.

Demazière, C., Pázsit, I., 2009. Numerical tools applied to power reactor noise analysis. Prog. Nucl. Energy 51 (1), 67–81. http://dx.doi.org/10.1016/j.pnucene.2008.01.010.

Dulla, S., E.H., M., Ravetto, P., 2008. The quasi-static method revisited. Prog. Nucl. Energy 50 (8), 908–920. http://dx.doi.org/10.1016/j.pnucene.2008.04.009.

Gammicchia, A., Santandrea, S., Zmijarevic, I., Sanchez, R., Stankovski, Z., Dulla, S., Mosca, P., 2020. A MOC-based neutron kinetics model for noise analysis. Ann. Nucl. Energy 137, 107070. http://dx.doi.org/10.1016/j.anucene.2019.107070.

Gelbard, E.M., 1960. Application of Spherical Harmonics Method to Reactor Problems. Technical Report No. WAPD-BT-20, Bettis Atomic Power Laboratory, West Mifflin, PA.

Ginestar, D., Verdú, G., Vidal, V., Bru, R., Marín, J., Munoz-Cobo, J., 1998. High order backward discretization of the neutron diffusion equation. Ann. Nucl. Energy 25 (1–3), 47–64. http://dx.doi.org/10.1016/S0306-4549(97)00046-7.

Gong, H., Chen, Z., Wu, W., Peng, X., Li, Q., 2021. Neutron noise calculation: A comparative study between SP3 theory and diffusion theory. Ann. Nucl. Energy 156, 108184. http://dx.doi.org/10.1016/j.anucene.2021.108184.

Hamilton, S.P., Evans, T.M., 2015. Efficient solution of the simplified PN equations. J. Comput. Phys. 284, 155–170. http://dx.doi.org/10.1016/j.jcp.2014.12.014.

Hauck, C., McClarren, R., 2010. Positive P_N closures. SIAM J. Sci. Comput. 32 (5), 2603–2626.

Larsson, V., Demazière, C., 2009. Comparative study of 2-group and diffusion theories for the calculation of the neutron noise in 1D 2-region systems. Ann. Nucl. Energy 36 (10), 1574–1587. http://dx.doi.org/10.1016/j.anucene.2009.07.009.

Lee, D., Kozlowski, T., Downar, T., 2015. Multi-group SP_3 approximation for simulation of a three-dimensional PWR rod ejection accident. Ann. Nucl. Energy 77, 94–100. http://dx.doi.org/10.1016/j.anucene.2014.10.019.

Lewis, E., Smith, M., Tsoulfanidis, N., Palmiotti, G., Taiwo, T., Blomquist, R., 2001. Benchmark specification for deterministic 2-D/3-D MOX fuel assembly transport calculations without spatial homogenization (C5G7 MOX). NEA/NSC 280.

McClarren, R.G., 2010. Theoretical aspects of the simplified Pn equations. Transport Theory Statist. Phys. 39 (2–4), 73–109. http://dx.doi.org/10.1080/00411450.2010.535088.

Mylonakis, A., Vinai, P., Demazière, C., 2021. CORE SIM+: A flexible diffusion-based solver for neutron noise simulations. Ann. Nucl. Energy 155, 108149. http://dx.doi.org/10.1016/j.anucene.2021.108149.

Olbrant, E., Larsen, E., Frank, M., Seibold, B., 2013. Asymptotic derivation and numerical investigation of time-dependent simplified equations. J. Comput. Phys. 238, 315–336. http://dx.doi.org/10.1016/j.jcp.2012.10.055.

Olmo-Juan, N., Demazière, C., Barrachina, T., Miró, R., Verdú, G., 2019. PARCS vs CORE SIM neutron noise simulations. Prog. Nucl. Energy 115, 169–180. http://dx.doi.org/10.1016/j.pnucene.2019.03.041.

Pázsit, I., Analytis, G.T., 1980. Theoretical investigation of the neutron noise diagnostics of two-dimensional control rod vibrations in a PWR. Ann. Nucl. Energy 7 (3), 171–183. http://dx.doi.org/10.1016/0306-4549(80)90082-1.

Rouchon, A., Sanchez, R., Zmijarevic, I., 2017a. The new 3-D multigroup diffusion neutron noise solver of APOLLO3® and a theoretical discussion of fission-modes noise. In: International Conference on Mathematics & Computational Methods Applied to Nuclear Science & Engineering (M&C 2017), Jeju, Korea, April. pp. 16–20.

Rouchon, A., Zoia, A., Sanchez, R., 2017b. A new Monte Carlo method for neutron noise calculations in the frequency domain. Ann. Nucl. Energy 102, 465–475. http://dx.doi.org/10.1016/j.anucene.2016.11.035.

Sanchez, R., 2019. On SPN theory. Ann. Nucl. Energy 129, 331–349. http://dx.doi.org/10.1016/j.anucene.2019.01.044.

Stacey, W.M., 2007. Nuclear Reactor Physics. Wiley, Weinheim, Germany, http://dx.doi.org/10.1002/9783527611041.

Vidal-Ferràndiz, A., Carreño, A., Ginestar, D., Demazière, C., Verdú, G., 2020a. Neutronic simulation of fuel assembly vibrations in a nuclear reactor. Nucl. Sci. Eng. 194 (11), 1067–1078.

Vidal-Ferràndiz, A., Carreño, A., Ginestar, D., Verdú, G., 2020b. FEMFFUSION: A finite element method code for the neutron diffusion equation. https://www.femffusion.imm.upv.es.

Vidal-Ferràndiz, A., no, A.C., Ginestar, D., Demazière, C., Verdú, G., 2020c. A time and frequency domain analysis of the effect of vibrating fuel assemblies on the neutron noise. Ann. Nucl. Energy 137, 107076. http://dx.doi.org/10.1016/j.anucene.2019.107076.

Vidal-Ferràndiz, A., no, A.C., Ginestar, D., Verdú, G., 2019a. A block arnoldi method for the SPN equations. Int. J. Comput. Math. 1–22. http://dx.doi.org/10.1080/00207160.2019.1602768.

Vidal-Ferràndiz, A., no, A.C., Ginestar, D., Verdú, G., 2019b. A block arnoldi method for the SPN equations. Int. J. Comput. Math. 1–22. http://dx.doi.org/10.1080/00207160.2019.1602768.

Viebach, M., Lange, C., Kliem, S., Demazière, C., Rohde, U., Hennig, D., Hurtado, A., 2019. A comparison between time domain and frequency domain calculations of stationary neutron fluctuations. In: Proc. Int. Conf. Mathematics and Computational Methods Applied to Nuclear Science and Engineering (M&C 2019). pp. 25–29.

Vinai, P., Demazière, C., Hou, J., Ivanov, K., 2019. Deterministic Time-Dependent Neutron Transport Benchmark Without Spatial Homogenization (C5G7-Td). Volume I: Kinetics Phase. Part B: Neutron Noise Simulation. Technical Report, Nuclear Energy Agency Organisation for Economic Co-operation and Development (NEA-OECD), Paris, France.

Vinai, P., Yi, H., Mylonakis, A., Demazière, C., Gasse, B., Rouchon, A., Zoia, A., Vidal-Ferràndiz, A., Ginestar, D., Verdú, G., Yamamoto, T., 2021a. Comparison of neutron noise solvers based on numerical benchmarks in a 2-D simplified UOX fuel assembly. In: Proceedings of the The International Conference on Mathematics and Computational Methods Applied to Nuclear Science and Engineering (M&C 2021). http://dx.doi.org/10.13182/M&C21-33625.

Vinai, P., Yi, H., Mylonakis, A., Demazière, C., Gasse, B., Rouchon, A., Zoia, A., Vidal-Ferràndiz, A., Ginestar, D., Verdú, G., et al., 2021b. Comparison of neutron noise solvers based on numerical benchmarks in a 2-D simplified UOX fuel assembly. Nucl. Sci. Eng..

Yi, H., Vinai, P., Demazière, C., 2021. On the simulation of neutron noise using a discrete ordinates method. Ann. Nucl. Energy 164, 108570. http://dx.doi.org/10.1016/j.anucene.2021.108570.